PROTEINS
STRUCTURE ■ FUNCTION ■ BIOINFORMATICS

Coarse-grained simulations of proton-dependent conformational changes in lactose permease

Yead Jewel, Prashanta Dutta, and Jin Liu*

School of Mechanical and Materials Engineering, Washington State University, Pullman, Washington 99164

ABSTRACT

During lactose/H^+ symport, the *Escherichia coli* lactose permease (LacY) undergoes a series of global conformational transitions between inward-facing (open to cytoplasmic side) and outward-facing (open to periplasmic side) states. However, the exact local interactions and molecular mechanisms dictating those large-scale structural changes are not well understood. All-atom molecular dynamics simulations have been performed to investigate the molecular interactions involved in conformational transitions of LacY, but the simulations can only explore early or partial global structural changes because of the computational limits (< 100 ns). In this work, we implement a hybrid force field that couples the united-atom protein models with the coarse-grained MARTINI water/lipid, to investigate the proton-dependent dynamics and conformational changes of LacY. The effects of the protonation states on two key glutamate residues (Glu325 and Glu269) have been studied. Our results on the salt-bridge dynamics agreed with all-atom simulations at early short time period, validating our simulations. From our microsecond simulations, we were able to observe the complete transition from inward-facing to outward-facing conformations of LacY. Our results showed that all helices have participated during the global conformational transitions and helical movements of LacY. The inter-helical distances measured in our simulations were consistent with the double electron-electron resonance experiments at both cytoplasmic and periplasmic sides. Our simulations indicated that the deprotonation of Glu325 induced the opening of the periplasmics side and partial closure of the cytoplasmic side of LacY, while protonation of the Glu269 caused a stable cross-domain salt-bridge (Glu130-Arg344) and completely closed the cytoplasmic side.

Proteins 2016; 00:000–000.

Key words: lactose/H+ symport; hybrid force field; LacY; salt-bridges; H-bonding.

INTRODUCTION

Transport of specific molecules across the cell membranes relies on the transmembrane proteins. The *Escherichia coli* lactose permease (LacY), a primary member of the major facilitator superfamily (MFS) proteins, plays essential roles in the active transport of galactosides across cell membranes.[1,2] LacY utilizes a proton gradient across the membrane ($\Delta\mu_{H^+}$) to drive the movement of galactosides through the membrane against the sugar concentration gradient. The coupled transport of galactoside and proton (lactose/H^+ symport) by LacY has become the prototype for studying MFS transport mechanisms and applications. For instance, a possible self-sustained micropump has been recently proposed based on mechanisms of lactose/H^+ symport in phloem.[3–5] As shown in Figure 1, LacY is complex in structure and composed of two pseudo-symmetric domains (N-terminal and C-terminal), each domain contains six transmembrane helices. The exact dynamics and structural changes of LacY during lactose/H^+ symport are largely unclear because of the complex nature of the process, but some simple and instructional schematics have been proposed based on the extensive experimental and simulation findings. For example as illustrated in Figure 1, a schematic similar to the work of Guan and Kaback[1] has been proposed. A complete cycle of lactose/H^+ symport

Additional Supporting Information may be found in the online version of this article.

Grant sponsor: US National Science Foundation; Grant number: CBET-1250107; Grant sponsor: the Extreme Science and Engineering Discovery Environment (XSEDE); Grant number: MSS150014.

*Correspondence to: Jin Liu; School of Mechanical and Materials Engineering, Washington State University, Pullman, WA 99164. E-MAIL: jin.liu2@wsu.edu

Received 12 January 2016; Revised 29 March 2016; Accepted 11 April 2016
Published online 18 April 2016 in Wiley Online Library (wileyonlinelibrary.com).
DOI: 10.1002/prot.25053

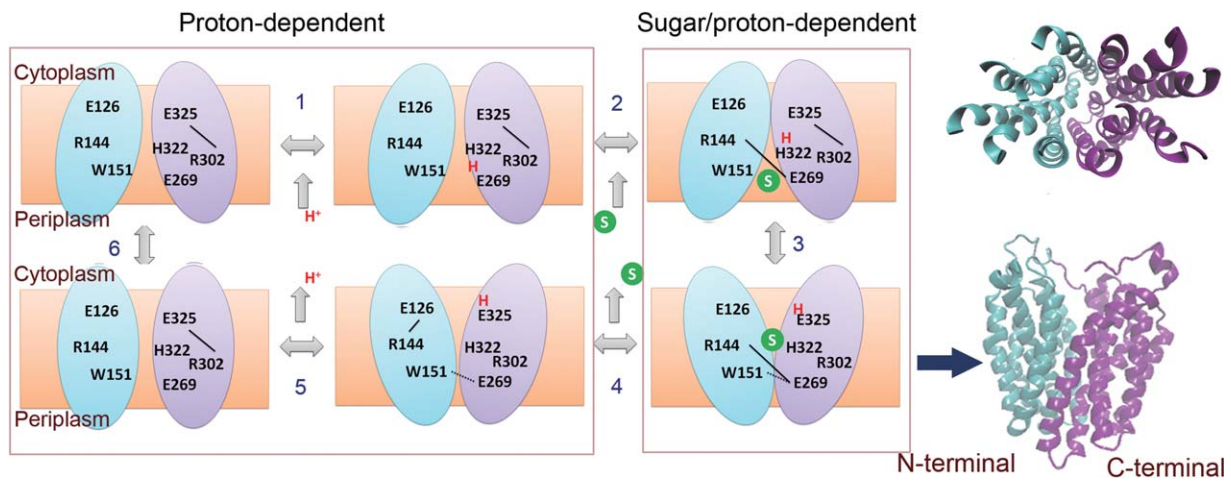

Figure 1

Schematic representation of the possible cycle of lactose/H^+ symport and LacY conformational changes according to the work of Guan and Kaback.[1] The important residues are labeled and the important salt-bridges (solid lines) and H-bonds (dashed lines) are indicated in the figure. Right figures show the new cartoon representation (cyan for N-terminal and purple for C-terminal domains) of inward-facing LacY. [Color figure can be viewed in the online issue, which is available at wileyonlinelibrary.com.]

may consist of the following six intermediate steps: (1) starting from the periplasmic-side open conformation, then LacY is protonated and the H^+ is thought to reside at Glu269 or shared between Glu269 and His322; (2) a sugar molecule binds to LacY from periplasmic side; (3) LacY undergoes a dramatic conformational transition from outward-facing to inward-facing states, and the H^+ is translocated to Glu325; (4) the sugar molecule is released from LacY to cytoplasmic side; (5) the H^+ is released from Glu325 to cytoplasm; (6) LacY undergoes a series of conformational changes and returns back to the outward-facing state. Finally the periplasmic side of LacY is open and ready to take next H^+, and then the cycle repeats. According to this schematic, the LacY conformational changes can be divided into proton-dependent with the absence of sugar and sugar/proton-dependent which involves the translocation of both sugar and H^+.

During lactose/H^+ symport the LacY protein experiences a sequence of large scale conformational transitions between inward-facing and outward-facing states. Each of these conformational transitions is a consequence of a complex interplay of numerous local interactions involving salt-bridges/H-bonds formations/breakages among side chains. So far, only the inward-facing conformation (shown in Fig. 1) was captured by the crystal structures.[6–8] The transition to outward-facing conformation has been explored by double electron–electron resonance (DEER)[9] and single-molecule fluorescence resonance energy transfer (FRET)[10] experiments. Experimental measurements of the distances between some labeled residue pairs indicated a decrease in cytoplasmic interhelical distances and an increase in periplasmic interhelical distances upon the binding of a sugar molecule. However, the local interactions which are critical to the conformational changes are dynamical and inaccessible to experiments. Molecular dynamics (MD) simulations are powerful in exploring detailed molecular scale interactions. A number of atomistic simulations[11–17] of LacY have been performed for understanding of the molecular mechanisms during lactose/H^+ symport process. For example, Yin et al.[11] have studied the effects of protonation states of Glu325 and Glu269 on the structural changes of a sugar-bounded LacY in ~10 ns simulations, but no significant structural changes were observed. Later, Holyoake and Sansom[12] captured the partial closure of the cytoplasmic side of LacY in ~50 ns simulations. In a more recent work, Andersson et al.[14] have performed ~100 ns simulations to investigate the effects of the protonation state of Glu325 and the type of lipid on the LacY transition from inward-facing to outward-facing conformation. Nevertheless, only partial closure of the cytoplamic side and no significant changes on the periplasmic side were observed in those simulations, likely because of the short period of the simulation times from the limit of the all-atom force fields. On the other hand, coarse-grained force fields, such as MARTINI[18,19] can significantly speedup the simulations but its applications are limited to cases where the conformational changes are of little importance because of the implementation of the elastic network. Therefore, a hybrid force field, in which the protein model is detailed enough to resolve the conformational features and the associated molecular interactions, while the environment (water and lipid) models are coarse-grained, will be ideal for resolving LacY structural changes during lactose/H^+ symport. Recently, such a hybrid force field, PACE has

been developed by Han et al.[20–25] In PACE, the united-atom-based protein model is coupled with the MARTINI water/lipid environment. It has been shown that the PACE force field was able to resolve multiple folding and unfolding events in several peptides[23] and capture the folding kinetics in small proteins[24] in microsecond simulations.

In this work, we investigate the LacY conformational changes and the associated molecular interactions through atomistic simulations in the hybrid PACE force field. Particularly we are interested in the proton-dependent structural changes with the absence of sugar molecule (shown in Fig. 1). We focus on the important roles of protonation states of two critical glutamate residues (Glu325 and Glu269) during the transition from inward-facing to outward-facing conformations. The implementation of hybrid force field enables us to perform microsecond simulations of LacY. Through our simulations we will discuss the both large-scale structural changes and local molecular interactions during the LacY conformational transitions.

MATERIALS AND METHODS

The PACE force field developed by Han et al.[20–25] was adopted in our simulations. Briefly PACE is a hybrid force field with a united-atom-based model (each heavy atom represents one site) for proteins coupled with the coarse-grained MARTINI[18,19] water and lipid model (four heavy atoms represent one site) to reduce the computational cost. In protein models, each heavy atom with the attached hydrogen atoms is generally modeled with one site, but the hydrogens on backbone and side-chain amide groups are also explicitly expressed for H-bonding. The total energy of the system can be expressed as

$$E = E_{\text{bond}} + E_{\text{angle}} + E_{\text{dihedral}} + E_{\text{improper}} + E_{\varphi,\psi,\chi_1} + E_{W-W} + E_{W-P} + E_{vdW} + E_{\text{polar}} \quad (1)$$

The first four terms account for bonded interactions connected with less than three covalent bonds, E_{φ,ψ,χ_1} is for interactions involved with rotamers of the backbone (ϕ and ψ) and the side chains (χ_1). The last four terms account for the nonbonded interactions including water–water interactions ($E_{W\text{-}W}$), water–protein interactions ($E_{W\text{-}P}$), interactions between nonpolar protein sites (E_{vdW}) and interactions between polar protein sites (E_{polar}). The nonbonded interactions are described by a Lennard-Jones (LJ) potential:

$$E_{ij} = \sum_{i \neq j} 4\epsilon_{ij} \left(\frac{\delta_{ij}^{12}}{r_{ij}^{12}} - \frac{\delta_{ij}^{6}}{r_{ij}^{6}} \right) \quad (2)$$

Here, ϵ_{ij} represents the inter-particle binding energy and δ_{ij} the van der Waals radius. r_{ij} is the distance between particles i and j. The equilibrium bond length and angle values were taken from the optimized geometries by quantum mechanics (QM) calculation. The dihedral parameters were obtained by fitting QM dihedral potential profiles of small molecules. Improper terms were used to maintain the planarity or chirality of groups. The interaction parameters for E_{φ,ψ,χ_1} were obtained through iterative equilibrium simulations against side-chain rotamer distributions and rotamer-dependent backbone conformations from a coil library. The parameters for water–protein interactions in Eq. (2) were optimized from fitting hydration free energies of 35 small organic molecules. E_{vdW} parameters were obtained on the basis of densities of liquid states and free energies of evaporation of eight organic compounds. The polar and charged sites interactions were optimized by fitting the PMFs from all-atom simulations with the OPLS-AA/L[26] force field in explicit water. Details on the modeling development and parameter optimization can be found in Refs.[22,24] It has been reported that using this hybrid force filed, simulations are able to resolve the multiple folding and unfolding events for small peptides,[23] as well as small proteins,[23] meanwhile the timescale explored in simulations is significantly increased compared with the all-atom simulations.

All simulations were performed using the modified version of NAMD 2.10.[27] PACE force field were adopted for protein, lipid, water, and ion molecules. The initial models were constructed using CHARMM-GUI.[28] Figure 2 illustrates our simulation system. As shown, our system contains 283 lipids after removal of the lipids overlapping

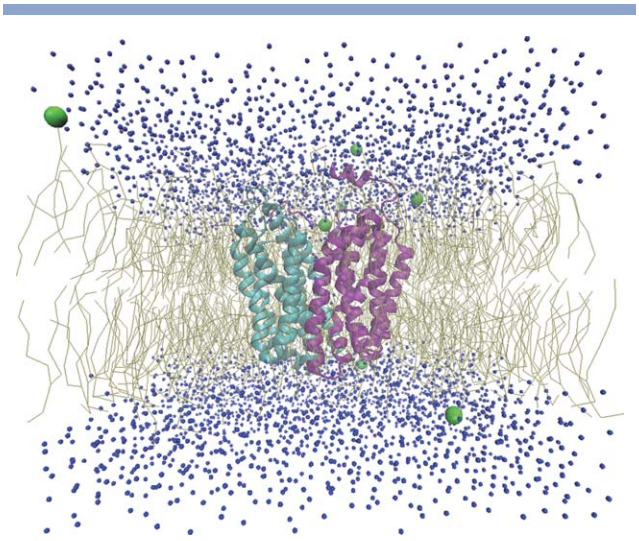

Figure 2

The illustration of the simulation box with LacY (new cartoon representation with cyan and purple colors for N-terminal and C-terminal domains) embedded in a POPE (line representation with golden color) lipid bilayer. Water and chloride molecules are represented by blue and green spheres respectively. [Color figure can be viewed in the online issue, which is available at wileyonlinelibrary.com.]

Table I
Summary of Simulation Systems

Simulation	Glu325	Glu269	Simulation time
LacY (325^H)	Protonated	Deprotonated	~3.2 μs
ApoLacY	Deprotonated	Deprotonated	~3.2 μs
LacY (269^H)	Deprotonated	Protonated	~3.2 μs

with the protein and around 5000 MARTINI water molecules. Small number of chloride ions (seven or eight) was added in our simulations to neutralize the entire system. The total system contained ~12,000 atoms with dimension of ~115 × 115 × 96 Å^3. The energy minimization and equilibration simulations have been performed with the harmonic constrains on the protein backbone α-carbons. In production simulations, the protein backbone constrains were released and 30 lipid head group phosphorus atoms at the top and bottom layers were randomly chosen and constrained in z direction to keep protein and lipid close to the center of the simulation domain. Periodic boundary conditions were applied in all three directions. The van der Waals interactions were calculated using LJ potential with a cutoff of 12 Å. Production simulations were carried out for ~3.2 μs using NPT ($T = 300$ K, $P = 1$ atm) ensembles. Since the protein force field is close to all-atom model, a time-step of 5 fs was chosen. However, the total number of atoms is significantly reduced compared with all-atom simulations because of the use of MARTINI water and lipids. Graphical software VMD has been used for analysis of atomic distances, salt-bridges, H-bonds and taking snap shots.

RESULTS

The protonation states of two key glutamate residues (Glu325 and Glu269) may play critical roles during the proton-dependent conformational changes of LacY.[1] Therefore, three model systems with different protonation states on Glu325 and Glu269 were simulated for ~3.2 μs as shown in Table I. In LacY (325^H) model, the Glu325 was protonated and Glu269 was deprotonated representing the stage right after the release of sugar molecular into the cytoplasm (see Fig. 1). In ApoLacY, both Glu325 and Glu269 were deprotonated and in LacY (269^H), Glu325 was deprotonated and Glu269 was protonated. The sugar substrate was absent in all simulations. Two independent simulations (sim 1 and sim 2) have been performed for cases of ApoLacY and LacY (269^H) for statistical consistency.

LacY side-chain dynamics and local interactions upon deprotonation of Glu325

The large-scale structural movements of LacY during proton-depending conformational changes are the accumulative consequence of a complex and dynamical formation/breakage of salt-bridges and H-bonds among side chains. It has been recognized that some key residues located around the hydrophilic binding site of LacY, such as Glu126 (helix IV), Arg144 (helix V), Trp151 (helix V), Glu325 (helix X), Arg302 (helix IX), His322 (helix X), and Glu269 (helix VIII),[1,6,29–34] actively participate the side-chain dynamics during lactose/H^+ symport. Among them, the salt-bridge between Arg144 and Glu126 has been studied from all-atom MD simulations[11,14] for its important roles on regulation of the movement of His322 and subsequent large scale conformational changes of LacY. Figure 3(a) shows the time evolution of the Arg144-Glu126 distance for both LacY (325^H) and ApoLacY cases at early stages (before 220 ns). In LacY (325^H) case a stable salt-bridge was present, but upon the deprotonation of Glu325 (ApoLacY) the salt-bridge between Arg144 and Glu126 was completely broken at ~200 ns (red line in sim 1) or partially weaken (orange line in sim 2) compared with LacY (325^H) case. These data agree well with the recent results from all-atom MD simulation from Ref. 14 as shown in Figure 3(c). And the weakening/breakage of Arg144-Glu126 salt-bridge has been postulated to correlate to the closure of the cytoplasmic side of the LacY.

Another important interaction driven by the deprotonation of Glu325 is the salt-bridge between Arg302 and Glu325.[29] As shown in Figure 3(b), a stable Arg302-Glu325 salt-bridge formed quickly after the deprotonation of Glu325 in ApoLacY cases (sim 1 and sim 2). When Glu325 was protonated, Arg302 and Glu325 tend to separate although an unstable and transient interaction was observed around 150 ns. The formation of Arg302-Glu325 salt-bridge also regulates the movement of His322 and the subsequent conformational changes LacY. Our results on Arg302-Glu325 salt-bridge dynamics are also consistent with the all-atom simulation data from Ref. 14 [Fig. 3(d)].

Large scale conformational changes because of the deprotonation of Glu325 and protonation of Glu269

There are many other salt-bridge and H-bond interactions besides the Arg144-Glu126 and Arg302-Glu325 salt-bridges discussed above. The overall results of these local interactions are the large-scale inter-helical movements and eventually the closure/opening of the cytoplasmic/periplasmic sides of the LacY. Previous simulations[11–14] can only capture the very early conformational changes because of the computational limitation (<100 ns in those simulations). On the other hand, it is possible to measure the LacY conformational changes experimentally. For example, Smirnova et al.[9] has quantitatively monitored the conformational changes of LacY through the measurements of the inter-helical

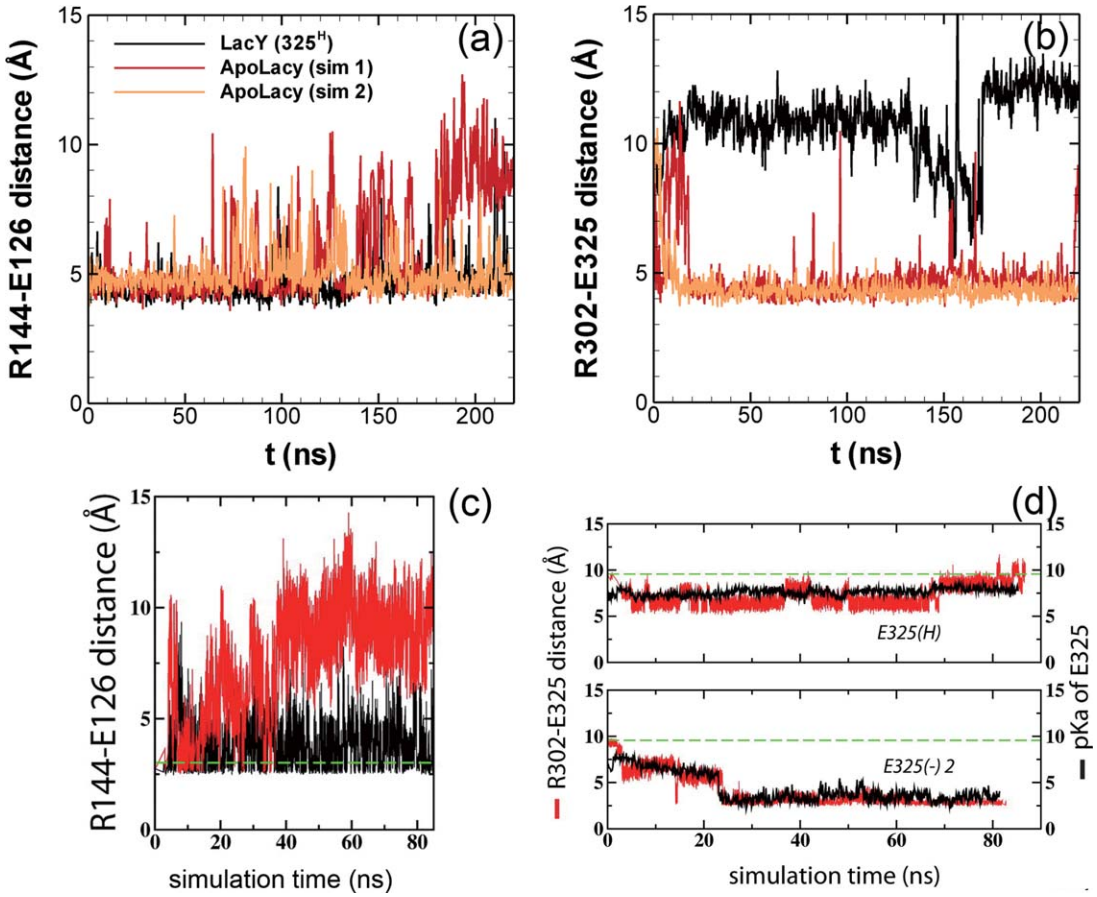

Figure 3

The time evolution of the inter-atomic R144-E126 distance (a) and R302-E325 distance (b) for cases with LacY (325^H) (black) and ApoLacY (red and orange) from our coarse-grained simulations. (c) The R144-E126 distance from all-atom simulations for LacY (325^H) (black) and ApoLacY (red). (d) The R302-E325 distance from all-atom simulations for LacY (325^H) (red line in top figure) and ApoLacY (red line in bottom figure). Figures (c) and (d) are reproduced with permission from Ref. 14. [Color figure can be viewed in the online issue, which is available at wileyonlinelibrary.com.]

distances using four-pulse DEER technique.[35,36] In the experiments, nine nitroxide-labeled paired-Cys replacements were attached to both cytoplasmic and periplasmic ends of helices on a wild-type LacY. Then the distance between each nitroxide-labeled pair was measured during the conformational transition from inward-facing to outward-facing state upon the binding of galactosidic or nongalactosidic sugars. From the measurements, the nitroxide-labeled pairs showed decreased distances ranging from 4 to 21 Å on the cytoplasmic side. On the periplasmic side, however, the nitroxide-labeled pairs exhibited increased distances ranging from 4 to 14 Å, clearly indicating a transition from inward-facing to outward-facing conformation. Particularly, from the distribution of the interspin distance between nitroxide-labeled Ile164 (Helix V) and Thr310 (Helix IX), the major population is around 35 Å when bonded with 4-nitrophenyl-α-D-glucopyranoside (NP*Glc*) and the population shifts to 45 Å upon binding with 4-nitrophenyl-α-D-galactopyranoside (NP*Gal*), clearly indicating the opening of the periplasmic side of LacY from 33 Å without sugar binding. On the cytoplasmic end, the distances between nitroxides bound at Arg73 (Helix III) and Ser401 (Helix XII) were measured. The distance population has been centered at 30 Å and 25/37 Å for cases when LacY was bounded with TDG and NP*Gal* respectively, evidently showing a closure of the cytoplasmic side from 46 Å without sugar binding.

For direct comparison with the experiments, we measure the backbone α-carbon distances between Ile164 and Thr310 at the periplasmic end and between Arg73 and Ser401 at the cytoplasmic side during the course of our simulations. Figure 4 shows the time evolutions of the respective distances for two cases (each case with two different realizations). As shown in Figure 4(a), when Glu325 was deprotonated (ApoLacY) the Ile164-Thr310 distance increased from 28 to 40 Å for both realizations showing the opening of the periplasmic side. Similar trend was also observed in cases when Glu269 was protonated. On the other hand, Figure 4(b) showed a clear

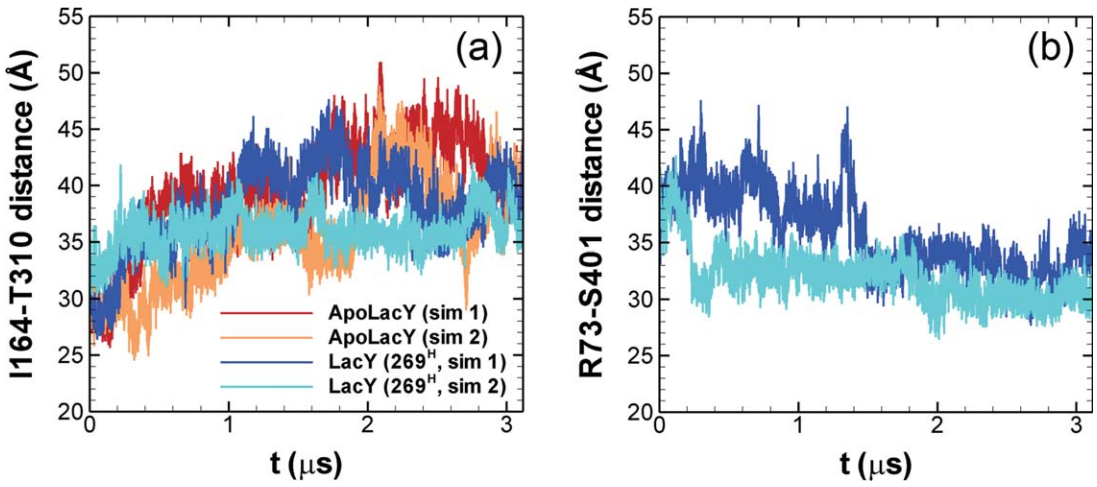

Figure 4

The time evolution of the inter-atomic (a) I164-T310 distance for cases with ApoLacY (red and orange) and LacY (269^H) (blue and cyan); and (b) R73-S401 distance for LacY (269^H). [Color figure can be viewed in the online issue, which is available at wileyonlinelibrary.com.]

decrease of the Arg73-Ser401 distance from 40 to 30 Å at the cytoplasmic side. The decreases were abrupt and occurred at different times for each realization, one at ~1.5 μs and one at very early time. Overall our simulation results are consistent with the experimental measurements and show dramatic inter-helical movements and structural reorganizations caused by the protonation/deprotonation of Glu325 and Glu269. Figure 5 (together with the movie for LacY (269^H) case in Supporting Information) shows the overall LacY structures at different protonation states illustrating the transition from inward-facing to outward-facing conformations from our simulations. Starting from the inward-facing conformation (crystal structure), deprotonation of Glu325 (ApoLacY) induces significant helical movement leading to the opening of the periplasmic end and partial closure of the cytoplasmic end (cylindrical or occluded structure), then protonation of Glu269 (LacY (269^H)) causes the complete closure of the cytoplasmic side (outward-facing structure).

The large-scale proton-depended conformational changes of LacY have also been studied by all-atom MD simulations.[11,14] Only partial closure of the cytoplasmic side and no appreciable changes on the periplasmic side were observed in those simulations. The partial closure of the cytoplasmic side has been attributed to the movement of some helices, such as helices V and VIII in Ref. 11 and helix IV in Ref. 14 However, as clearly shown in Figures 4 and 5 from our simulations, we observed both the opening of the periplasmic side and full closure of

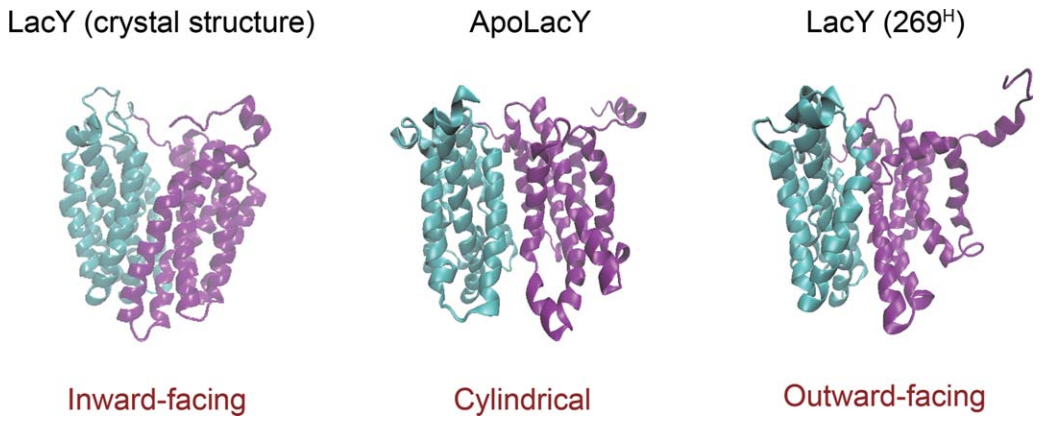

Figure 5

The conformational changes in LacY at different protonation states. (left) inward-facing conformation from crystal structure; (middle) a transition state conformation (cylindrical) because of the deprotonation of E325; (right) and outward-facing conformation because of the protonation of E269.

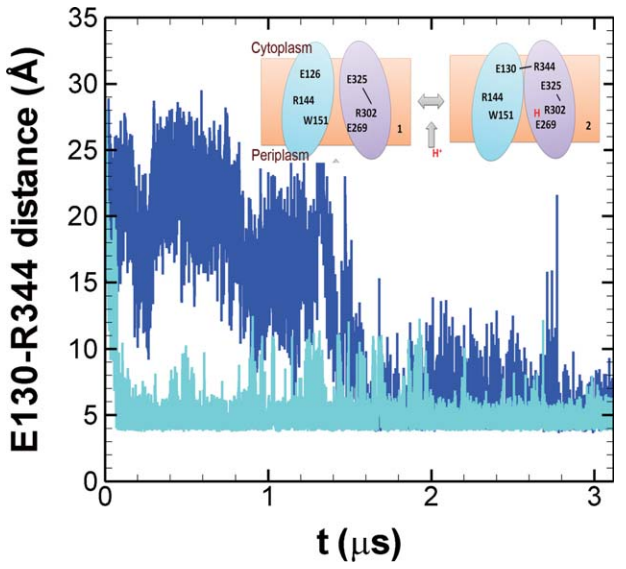

Figure 6

The time evolution of the inter-atomic E130-R344 distance for LacY (269^H). (E130 is on helix IV and R344 is on helix XI). [Color figure can be viewed in the online issue, which is available at wileyonlinelibrary.com.]

the cytoplasmic side of LacY. And all helices have participated the global transition from inward-facing to outward-facing conformations. The periplasmic side opens in both ApoLacY and LacY (269^H) cases and is probably caused by the dissociation of the sugar molecule. The cytoplasmic side partially closes in ApoLacY resulting an intermediate cylindrical state but completely closes in LacY (269^H) leading to the final outward-facing state. We have explored the LacY (269^H) case and found that a salt-bridge between Glu130 and Arg344 formed in both realizations and the salt-bridge was quite stable during the course of the simulations as shown in Figure 6. Glu130 resides on helix IV in C-domain and Arg344 on helix XI in N-domain. We also notice that the formation of this salt-bridge coincides with the closing movement between Arg73 and Ser401 as shown in Figure 4(b). Therefore, this cross-domain interaction between Glu130 and Arg344 may play key roles for complete closure of cytoplasmic. Furthermore, in our simulations the Glu130-Arg344 salt-bridge forms only in LacY (269^H) case when Glu269 is protonated. When Glu269 is deprotonated (ApoLacY), no such stable salt-bridges were identified.

DISCUSSION AND CONCLUSIONS

In this work MD simulations have been performed to investigate the proton-dependent conformational changes of LacY protein during lactose/H^+ symport. A hybrid PACE force field, where the united atom protein model is coupled with MARTINI water/lipid models, was adopted in our simulations. This force field enables us to explore the large-scale LacY conformational changes in microseconds (~3.2 μs), meanwhile retaining the detailed molecular scale interactions. Three cases with the absence of sugar molecule: LacY (325^H), ApoLacY, and LacY (269^H), have been studied based on the protonation states of two key glutamic acids (Glu325 and Glu269).

We first investigate the evolution of two key local interactions (salt-bridges Arg144-Glu126 and Arg302-Glu325) because of the deprotonation of Glu325 (LacY (325^H) to ApoLacY) which have been identified from previous all-atom simulation. During the early stage (within 220 ns), our results are consistent with all-atom simulation data validating our simulations. Then, we investigate the large scale inter-helical movements of LacY, and for the first time we are able to capture an overall transition from inward-facing to outward facing state from molecular simulations. Deprotonation of Glu325 induces both the opening of the periplasmic side and partial closure of the cytoplasmic side, then protonation of Glu269 results in a formation of a stable cross-domain salt-bridge (Glu130-Arg344) and completely closes the cytoplasmic side of LacY. As illustrated in Figure 1, binding of sugar molecule in LacY can also induce similar inward-facing to outward-facing transitions. It will be interesting to include the sugar molecule in the simulations to complete the cycle in future work. Finally as mentioned in Ref. 24, because of the coarse-graining of water/lipid and simplification of the protein–protein and protein–solvent interactions in PACE, the kinetics of protein dynamics may be significantly faster than experiments. Therefore, we expect that the real conformational transitions of LacY occur in a much larger time scale than our simulation times. Nevertheless, our simulations provide important information on LacY protein structural changes as well as dynamic interactions during lactose/H^+ symport.

REFERENCES

1. Guan L, Kaback HR. Lessons from lactose permease. Annu Rev Biophys Biomol Struct 2006; 35:67–91.
2. Kaback HR. The lactose permease of *Escherichia coli*a paradigm for membrane-transport proteins. Biochim Biophys Acta 1992; 1101: 210–213.
3. Sze T-kJ, Liu J, Dutta P. Numerical modeling of flow through phloem considering active loading. J Fluids Eng 2014; 136:021206
4. Sze T-kJ, Liu J, Dutta P. Study of protein facilitated water and nutrient transport in plant phloem. J Nanotechnol Eng Med 2014; 4:031005
5. Sze T-kJ, Liu J, Dutta P. Modeling and design of light powered biomimicry micropump utilizing transporter proteins. J Micromech Microeng 2015; 25:065009
6. Abramson J, Smirnova I, Kasho V, Verner G, Kaback HR, Iwata S. Structure and mechanism of the lactose permease of *Escherichia coli*. Science 2003; 301:610–615.

7. Guan L, Mirza O, Verner G, Iwata S, Kaback HR. Structural determination of wild-type lactose permease. Proc Natl Acad Sci U S A 2007; 104:15294–15298.
8. Chaptal V, Kwon S, Sawaya MR, Guan L, Kaback HR, Abramson J. Crystal structure of lactose permease in complex with an affinity inactivator yields unique insight into sugar recognition. Proc Natl Acad Sci U S A 2011; 108:9361–9366.
9. Smirnova I, Kasho V, Choe J-Y, Altenbach C, Hubbell WL, Kaback HR. Sugar binding induces an outward-facing conformation of LacY. Proc Natl Acad Sci U S A 2007; 104:16504–16509.
10. Majumdar DS, Smirnova I, Kasho V, Nir E, Kong X, Weiss S, Kaback HR. Single-molecule FRET reveals sugar-induced conformational dynamics in LacY. Proc Natl Acad Sci U S A 2007; 104: 12640–12645.
11. Yin Y, Jensen MO, Tajkhorshid E, Schulten K. Sugar binding and protein conformational changes in lactose permease. Biophys J 2006; 91:3972–3985.
12. Holyoake J, Sansom MSP. Conformational change in an MFS protein: MD simulations of LacY. Structure 2007; 15:873–884.
13. Jensen MO, Yin Y, Tajkhorshid E, Schulten K. Sugar transport across lactose permease probed by steered molecular dynamics. Biophys J 2007; 93:92–102.
14. Andersson M, Bondar A-N, Freites JA, Tobias DJ, Kaback HR, White SH. Proton-coupled dynamics in lactose permease. Structure 2012; 20:1893–1904.
15. Bennett M, D'Rozario R, Sansom MSP, Yeagle PL. Asymmetric stability among the transmembrane helices of lactose permease. Biochemistry 2006; 45:8088–8095.
16. Klauda JB, Brooks BR. Sugar binding in lactose permease: anomeric state of a disaccharide influences binding structure. J Mol Biol 2007; 367:1523–1534.
17. Pendse PY, Brooks BR, Klauda JB. Probing the periplasmic-open state of lactose permease in response to sugar binding and proton trans location. J Mol Biol 2010; 404:506–521.
18. Marrink SJ, de Vries AH, Mark AE. Coarse grained model for semi-quantitative lipid simulations. J Phys Chem B 2004; 108:750–760.
19. Marrink SJ, Risselada HJ, Yefimov S, Tieleman DP, de Vries AH. The MARTINI force field: coarse grained model for biomolecular simulations. J Phys Chem B 2007; 111:7812–7824.
20. Han W, Wu Y-D. Coarse-grained protein model coupled with a coarse-grained water model: molecular dynamics study of polyalanine-based peptides. J Chem Theory Comput 2007; 3:2146–2161.
21. Han W, Wan C-K, Wu Y-D. Toward a coarse-grained protein model coupled with a coarse-grained solvent model: solvation free energies of amino acid side chains. J Chem Theory Comput 2008; 4:1891–1901.
22. Han W, Wan C-K, Jiang F, Wu Y-D. PACE force field for protein simulations. 1. Full parameterization of Version 1 and verification. J Chem Theory Comput 2010; 6:3373–3389.
23. Han W, Wan C-K, Wu Y-D. PACE force field for protein simulations. 2. Folding simulations of peptides. J Chem Theory Comput 2010; 6:3390–3402.
24. Han W, Schulten K. Further optimization of a hybrid united-atom and coarse-grained force field for folding simulations: improved backbone hydration and interactions between charged side chains. J Chem Theory Comput 2012; 8:4413–4424.
25. Wan C-K, Han W, Wu Y-D. Parameterization of PACE force field for membrane environment and simulation of helical peptides and helix–helix association. J Chem Theory Comput 2012; 8:300–313.
26. Kaminski GA, Friesner RA, Tirado-Rives J, Jorgensen WL. Evaluation and reparametrization of the OPLS-AA force field for proteins via comparison with accurate quantum chemical calculations on peptides. J Phys Chem B 2001; 105:6474–6487.
27. Phillips JC, Braun R, Wang W, Gumbart J, Tajkhorshid E, Villa E, Chipot C, Skeel RD, Kale L, Schulten K. Scalable molecular dynamics with NAMD. J Comput Chem 2005; 26:1781–1802.
28. Jo S, Kim T, Iyer VG, Im W. Software news and updates—CHARNIM-GUI: a web-based graphical user interface for CHARMM. J Comput Chem 2008; 29:1859–1865.
29. Sahin-Toth M, Kaback HR. Arg-302 facilitates deprotonation of Glu-325 in the transport mechanism of the lactose permease from *Escherichia coli*. Proc Natl Acad Sci U S A 2001; 98:6068–6073.
30. He MM, Kaback HR. Interaction between residues Glu269 (helix VIII) and His322 (helix X) of the lactose permease of *Escherichia coli* is essential for substrate binding. Biochemistry 1997; 36:13688–13692.
31. Sahin-Toth M, Karlin A, Kaback HR. Unraveling the mechanism of the lactose permease of *Escherichia coli*. Proc Natl Acad Sci U S A 2000; 97:10729–10732.
32. Frillingos S, Gonzalez A, Kaback HR. Cysteine-scanning mutagenesis of helix IV and the adjoining loops in the lactose permease of *Escherichia coli*: Glu126 and Arg144 are essential. Biochemistry 1997; 36: 14284–14290.
33. Smirnova I, Kasho V, Sugihara J, Choe J-Y, Kaback HR. Residues in the H+ translocation site define the pK(a) for sugar binding to LacY. Biochemistry 2009; 48:8852–8860.
34. Mirza O, Guan L, Verner G, Iwata S, Kaback HR. Structural evidence for induced fit and a mechanism for sugar/H+ symport in LacY. Embo J 2006; 25:1177–1183.
35. Pannier M, Veit S, Godt A, Jeschke G, Spiess HW. Dead-time free measurement of dipole–dipole interactions between electron spins. J Magn Reson 2000; 142:331–340.
36. Jeschke G. Distance measurements in the nanometer range by pulse EPR. Chemphyschem 2002; 3:927–932.